Tikrit Journal of Engineering Sciences (2025); 32(3): 2128
DOI: http://doi.org/10.25130/tjes.32.3.25

IRAQI Academic Scientific Journals

ISSN: 1813-162X (Print); 2312-7589 (Online)
Tikrit Journal of Engineering Sciences
available online at: http://www.tj-es.com

TJES Tikrit Journal of Engineering Sciences

Temperature Analysis of Three-Phase 15kW Switched Reluctance Motor Based on Motor_CAD ANSYS Software

Hussein Ali Bardan *, *Abdalrahman Ataalla*, *Aymen Jalil Abdulelah*, *Ahmed Hikmat Saeed*, *Munther Naif Thiyab*

Department of Computer Engineering Techniques, College of Technical Engineering, University of Al-Maarif, Al Anbar,31001, Iraq.

Keywords:
SRM; RMXprt; Motor_CAD; LPTN; Temperature analysis; Spray cooling; Water jacket cooling.

Highlights:

- *Temperature analysis of three-phase, 15kW, 18/12 stator/rotor poles SRM.*
- *Cooling methods include pray cooling, water jacket, and different loading conditions.*
- *Analysis of the efficiency of SRM with changing the number of phases.*
- *ANSYS Electronic Desktop 2018 contains RMXprt software.*
- *The SRM model in Motor-CAD was created in Motor-CAD version 14.1.2 by RMXprt software.*

ARTICLE INFO

Article history:

Received	09 Apr. 2024
Received in revised form	19 July 2024
Accepted	21 Aug. 2024
Final Proofreading	14 Aug. 2025
Available online	28 Aug. 2025

Citation: Bardan HA, Ataalla A, Abdulelah AJ, Saeed AH, Thiyab MN. **Temperature Analysis of Three-Phase 15kW Switched Reluctance Motor Based on Motor_CAD ANSYS Software**. *Tikrit Journal of Engineering Sciences* 2025; **32**(3): 2128. http://doi.org/10.25130/tjes.32.3.25

*Corresponding author:
Hussein Ali Bardan
Department of Computer Engineering Techniques, College of Technical Engineering, University of Al-Maarif, Al Anbar,31001, Iraq.

Abstract: An electrical motor that utilizes the principle of magnetic reluctance to generate motion is called a Switched Reluctance Motor (SRM). It has a simple structure with a stator and rotor having salient poles and winding only in the stator. SRMs don't have permanent magnets on the rotor, unlike traditional motors. This paper introduces the temperature analysis of a three-phase, 15kW, 18/12 stator/rotor poles SRM using RMXprt (analytical software, and Motor_CAD software, which is based on LPTN (Lumped Parameter Thermal Network). Cooling strategies, such as water, fins, and spray, are examined to mitigate temperature rise. The analysis encompasses varying load conditions, which are also considered, allowing for a comprehensive evaluation of their temperature effects on the SRM. Motor losses, such as mechanical losses, copper losses, and core losses, are considered the source of SRM heat, which was determined by RMXprt software. Furthermore, this paper presents the efficiency analysis of SRM by changing the number of phases. The temperature analysis by Motor_CAD presents the distribution of temperature on various parts of the motor, such as housing, shaft, rotor yoke, rotor poles, stator yoke, stator poles, and stator winding. The results of this analysis aim to contribute valuable information for optimizing the design and operation of SRM, particularly in terms of thermal management, efficiency, and overall reliability.

تحليل درجة الحرارة لمحرك ممانعة تبديل ثلاثي الطور بقدرة ١٥ كيلو واط استنادًا إلى برنامج Motor_CAD ANSYS

حسين علي بدران، عبدالرحمن عطاالله، ايمن جليل عبدالله، احمد حكمت سعيد، منذر نايف ذياب
قسم تقنيات هندسة الحاسوب، كلية الهندسة التقنية، جامعة المعارف / الرمادي - العراق.

الخلاصة

يسمى المحرك الكهربائي الذي يستخدم مبدأ الممانعة المغناطيسية لتوليد الحركة بمحرك المعاوقة المبدلة (SRM). يتمتع بتركيب بسيط مع وجود اقطاب بارزة في الجزء الثابت والدوار وملفات فقط في الجزء الثابت. لا يحتوي محرك المعاوقة المبدلة على مغناطيس دائم في الجزء الدوار على عكس المحركات التقليدية. يقدم هذا البحث تحليل درجة الحرارة لمحرك المعاوقة المبدلة ثلاثي الاطوار بقدرة ١٥ كيلوواط باقطاب /١٢١٨ للجزء الثابت على الدوار باستخدام برنامج RMXprt (وهو برنامج تحليلي) وبرنامج Motor_CAD الذي يعتمد على شبكة العناصر الحرارية المجمعة. تم فحص استراتيجيات التبريد مثل التبريد بالماء والزعانف والرش للتقليل من ارتفاع درجة الحرارة. يشمل التحليل ظروف الحمل المتغيرة أيضا مما يسمح بتقييم شامل لتاثيرات درجة الحرارة على محرك المعاوقة المبدلة. يتم اعتبار خسائر المحرك مثل الخسائر الميكانيكية والخسائر النحاسية والخسائر الأساسية مصدر حرارة محرك المعاوقة المبدلة والتي تم حسابها بواسطة برنامج RMXprt علاوة على ذلك يقدم هذا البحث تحليل كفاءة محرك المعاوقة المبدلة من خلال تغيير عدد الأطوار. ينتج التحليل الحراري لبرنامج Motor_CAD عن تقديم توزيع درجة الحرارة على أجزاء محتلفة من المحرك مثل الهيكل والعمود وحلقة الدوار واقطاب الدوار وحلقة الثابت واقطاب الجزء الثابت وملفات الجزء الثابت. تهدف نتائج هذا التحليل الى المساهمة بمعلومات قيمة لتحسين تصميم وتشغيل محرك المعاوقة المبدلة بشكل خاص من تنظيم درجة الحرارة والكفاءة والموثوقية العامة.

الكلمات الدالة: SRM؛ RMXprt؛ Motor_CAD؛ LPTN؛ تحليل درجة الحرارة؛ تبريد الرش؛ تبريد سترة الماء.

1.INTRODUCTION

A switched reluctance motor (SRM) is electrical motor that operates based on the principle of minimum reluctance. The SRM is used in various applications, such as regenerative braking systems, renewable energy, robotics, aerospace, home appliances, industrial drives, automotive systems, home appliances, HVAC systems, and high-speed applications due to its several advantages, such as high efficiency, fault tolerance, wide speed range, high power density, and simple construction. However, the housing of the motor and coil temperature rise may be high when operating for a long time or at high power. Also, the mechanical losses increase at high speed because both the rotor and stator are salient poles [1]. To solve this problem, several methodologies have been used in previous studies for temperature analysis. Nasim used 3D FEA to calculate the distribution of temperature in different areas of a 10kW, 12/8 double stator SRM utilizing the liquid cooling approach [2]. CFD with 3D FEA was used by Elhomdy et al. to calculate the distribution temperature in motor sections utilizing the cooling approach via a water jacket on a 75kW, three-phase 72/48 SRM. The findings established the presence of greater temperatures in the motor winding [3]. Pavan used CFD software to evaluate the distribution of heat in the rotor and stator of a three-phase 6/4 SRM in a 3D FEM steady-state analysis [4]. Motor_CAD was used by Bieńkowski et al. to calculate the temperature for various stator/rotor pole combinations of 10/8, 8/6, and 6/4, and FEA to calculate torque [5]. Chiu et al. used Solidworks software to build the model of an 18/12 SRM, three-phase, 30kW, as well as JMAG and Ansys Fluent to evaluate electromagnetic torque and temperature distribution, respectively. The findings revealed that cooling by water increased the temperature of SRM [6]. Hung used Maxwell Ansys to calculate the losses of the motor and workbench Ansys to calculate the distribution of temperature in SRM for the rotor and stator windings for a 12/8 SRM, 110kW [7]. Jang et al. examined a 12/8 SRM, 3kW motor by utilizing JMAG Designer software to quantify the losses of iron and computational fluid dynamics (CFD) to assess the distribution temperature of the motor [8]. Reis et al. used Maxwell2D software to measure motor flux linkage, current, and torque on a three-phase 2kW, 6/4SRM, and workbench software to calculate the rise in the internal temperature, which is greatest in the winding [9]. Kasprzak et al. used Motor-CAD Ansys to study a 24/16 SRM, 60kW, to evaluate the distribution of temperature based on LPTN with varying values of speed to predict temperature rise in various machine parts [10]. Vijayakumar et al. utilized FEA to evaluate torque, inductance, and temperature in a three-phase 6/4 SRM. The authors proved that the SRM heat distribution was enhanced using SMC as the magnetic core of the SRM [11]. Nasab et al. used FEA to calculate motor losses in their analysis of a four-phase, 8/6 pole SRM. The authors also utilized CFD Ansys to create a 3D thermal model that predicted the temperature on the SRM housing and the distribution of temperature on the surface to predict a fault in the heat transfer in SRM [12]. Abunike et al. examined a 12/8 SRM, three-phase 4kW using workbench software to calculate the distribution of the temperature in the housing, stator, rotor, and winding, and utilized the water jacket cooling approach. They also used Maxwell2D software to calculate core losses, torque, copper losses, and flux [13]. Yan et al. investigated an 8/6 SRM four-phase using Flux2D FEA software, changing the values of speed to calculate magnetic flux density, iron losses, and temperature in the presence of two

magnetic distributions of poles. After analyzing the results, it was found that the iron loss in the machine was greater with the NNSN-SSNS pole magnetic distribution than the NNNN-SSSS distribution. The SRM 2D FEA temperature field model was then developed and evaluated. The experimental data showed that the temperature rise was consistent with that of the measurement platform [14]. Sun et al. analyzed a 12/8 SRM, three-phase, 2.2 kW by utilizing 2D FEA in transient analysis and ANSYS software. The orthogonal decomposition approach was used to analyze iron losses. To supply the total losses of the motor, the external circuit was used. The results showed that the proposed approach was correct and feasible [15]. Kartigeyan and Ramaswamy used M400-50A, DI MAX-M19, and DI MAX-M15 steel types for testing 12/8 SRM, three-phase, 1.5kW by utilizing two-dimensional (2D) FEA. To evaluate core and copper losses, the results showed that DI MAX-M15 had lower losses than other steel materials. The authors utilized experimental measurements to compare results with an acceptable error rate [16]. Kocan and Rafajdus analyzed a 6/4 SRM, three-phase, 1.5 kW with different values of speed based on Matlab/Simulink to compute losses, torque, efficiency, and torque ripple. Torque ripple increased directly at speeds surpassing 75,000 rpm. By changing the control method, this torque ripple may be reduced. As speed increased, the winding losses decreased. There were rises in iron losses over 25,000 rpm; however, the increase was not significantly higher than 75,000 rpm. Mechanical losses are the most common; however, they were determined only roughly, and more exact values may be acquired by measuring [17]. Kocan et al. analyzed a 6/4 SRM, three-phase, 1.7 kW system using Simplorer and Maxwell2D software, altering the geometry of the rotor in comparison to the original design. The redesigned rotor has shorter and wider teeth compared to the previous design. The results clarified that the alteration in geometry of the rotor leads to a high value for average torque; however, torque ripple and losses are higher [18]. Al-Farhan and Yehya reviewed techniques for improving the geometric design of SRM to enhance key objectives, such as minimizing radial force, reducing torque ripple, increasing torque, and enhancing efficiency. The review covers the method utilized to optimize the structure of SRM, including changing the number and shape of rotor and stator poles, modifying the stator windings' shape, changing the phase number, and modifying the air gap size [19]. Alattar and Alsammak analyzed a six-phase induction motor using different kinds of control strategies utilized to enhance motor operating, such as SMC, DTC, INFOC, and FOC [20]. Abbas et al. conducted an analysis and evaluation of the output of a three-phase induction motor operating on a balanced power source. They compared it with the "single-phase" condition. The MATLAB / SIMULINK software was utilized for the simulation. Additionally, the effects of single-phasing on the performance of the three-phase induction motor were proposed to restore the system [21]. Mahmmoud et al. developed a system that optimizes solar energy use by combining DC/AC and DC/DC converters and inverters with PV cells. The authors used an induction motor as the load, controlled by a DC/DC converter and MPPT using the Incremental Conductance method. The system also applied Sine Pulse Width Modulation (SPWM) with a three-level inverter. The simulations showed improved performance [22]. The present study aims to conduct a temperature analysis on 18/12, 15kW SRM, combining two software tools, RMXprt and Motor_CAD, under different loading conditions, and to study the effect of using different cooling approaches (spray cooling and water jacket cooling. Also, the efficiency of SRM with changes in the number of phases was analyzed.

2.THEORETICAL BACKGROUND OF SRM

Figure 1 illustrates the distribution of losses in SRM, which are considered a source of heat inside this motor [1].

Fig. 1 Distribution of the Losses in SRM.

Losses in SRM can contribute to temperature rise. Frictional and windage losses, core losses, and copper losses are common sources of heat. Frictional and windage losses are mechanical losses due to friction in the bearings. While windage losses result from air resistance of rotating components, core losses result from hysteresis and eddy current effects in the iron core of the motor, and copper losses occur in the windings due to resistance [1]. The core loss (P_{core}(W)) is calculated using the following equation:

$$\mathbf{P_{core} = P_{ex} + P_e + P_h} \quad \mathbf{(1)}$$

where P_{ex}(W), P_e(W), and P_h (W) denote excess loss, eddy current loss, and hysteresis loss, respectively. The copper losses (P_{cu} (W)) are calculated using the following equation:

$$\mathbf{P_{cu} = I^2Rq = I^2q\rho\frac{l}{s}} \quad \mathbf{(2)}$$

where R(Ω) is the stator resistance per phase, q is the phase number, I (A) is the RMS phase current, ρ is the resistivity of the conductor, ℓ is the length of the conductor, and s is the cross-sectional area of the conductor. For small SRM machines, the following equation is used for computing friction and windage loss(P_{fw}(W)):

$$\mathbf{P_{fw} = 2D^3Ln^3 \times 10^{-6} + G_n k_{fb} \times 10^{-3}} \quad \mathbf{(3)}$$

where D (in meters) is the outer diameter of the rotor, L is the stack length in meters, n is the motor speed in rpm, G_n is the rotor weight in kg, and k_{fb} is the frictional loss coefficient [1]. The total losses (P_T (W)) are calculated from [23]:

$$\mathbf{P_T = P_{cu} + P_{core} + P_{fw}} \quad \mathbf{(4)}$$

The resistivity of the conductor(ρ), as a function of temperature, is calculated from [1]:

$$\mathbf{\rho = \rho_0[1 + \alpha(T - T_0)}} \quad \mathbf{(5)}$$

where T_o and T are the initial and final temperatures in Kelvin, respectively, ρ_o is the initial resistivity, and α is the temperature coefficient of the material. The transfer of heat is categorized into three kinds based on the principle of heat transmission: radiation, convection, and conduction. The main path for heat flow in this motor is clarified in Fig. 2 [1].

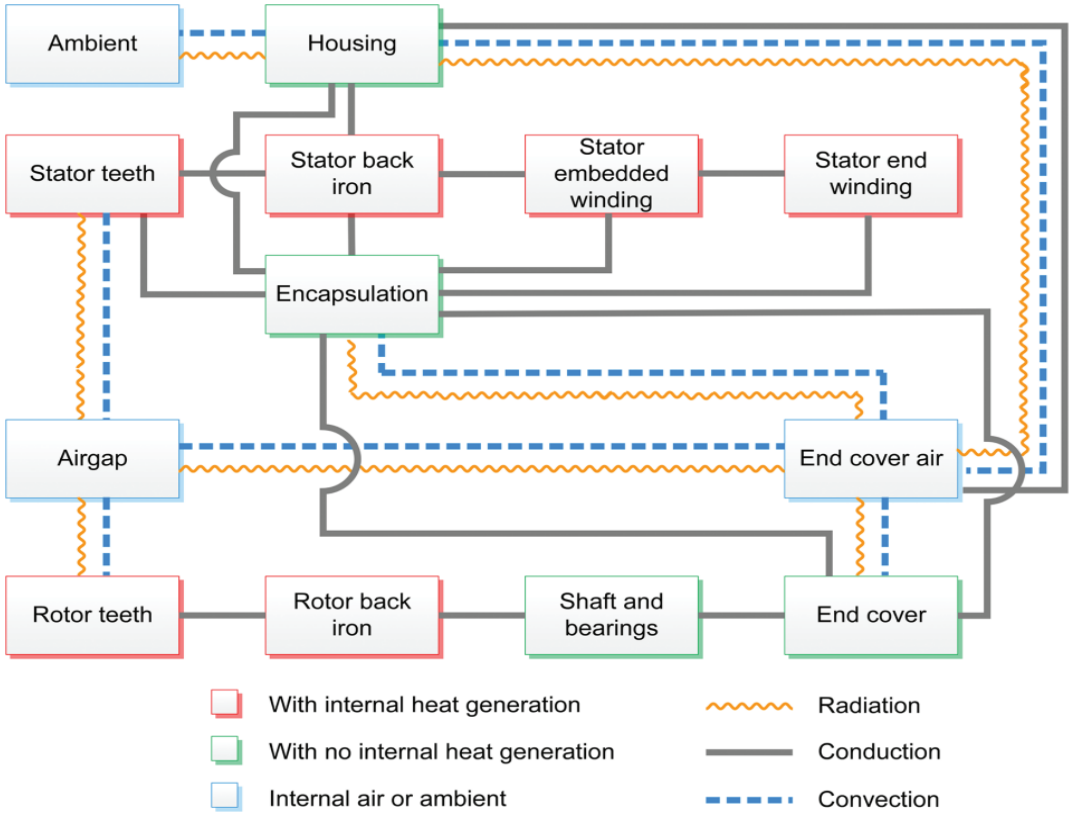

Fig. 2 The Main Path of Heat Transfer in SRM.

The equation for computing heat radiation (Q_{rad}) is given by:

$$\mathbf{Q_{rad} = A_s\sigma\varepsilon(T^4 - T_{Surr}{}^4)} \quad \mathbf{(6)}$$

where A_s is the radiating surface area, σ (5.67×10^{-8} W/(m² K⁴) is the Stefan-Boltzmann law, ε (between 0 and 1) is the emissivity, and T_{surr} is the surrounding surface temperature. The equation for computing the heat convection (Q_{conv}) is given by:

$$\mathbf{Q_{conv} = A_s h(T_s - T_\infty)} \quad \mathbf{(7)}$$

where A_s is the surface area in which the convection heat transfer happens, h is the convection heat transfer coefficient (W/(m² K)), T_s and T_∞ are the surface and fluid temperatures, respectively. The equation for computing heat conduction (Q_{cond}) is given by:

$$\mathbf{Q_{cond} = -AK\frac{d_T}{d_x}} \quad \mathbf{(8)}$$

where Q_{cond} is the heat conduction, A is the heat transfer area, k is the thermal conductivity

coefficient for the material (W/(m k)), and $\frac{d_T}{d_x}$ is the temperature gradient, i.e., the rate of varying T with x [24].

3.MODELING AND SIMULATION OF SRM BY RMXPRT AND MOTOR-CAD

RMXprt Design is a template-based electrical machine design tool that allows for quick, analytical estimates of machine performance, as well as the generation of 2-D and 3-D geometry for comprehensive finite element simulations in Maxwell ANSYS. Motor-CAD is software that enables engineers to perform temperature analyses of diverse motor types, which uses a 3D lumped model parameter circuit that can be utilized to simulate electrical machines in both steady-state and transient temperature states. The process involves combining the two software by exporting RMXprt data. This process includes the following steps: Get initial thermal data (e.g., losses) from RMXprt, input to Motor-CAD: Use RMXprt data in Motor-CAD for detailed thermal analysis, and analyze in Motor-CAD: Perform a comprehensive thermal analysis. The rated voltage is 300 V, the rated speed is 3000 rpm, the rated output power is 15 kW, and other specifications of the motor that is utilized in RMXprt software are clarified in Table 1, which were taken from [25]. Figure 3 illustrates the sectional view of SRM by RMXprt.

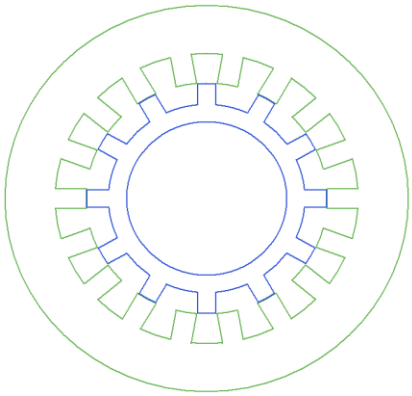

Fig. 3 Sectional View of SRM by RMXprt.

Table 1 SRM Specification.

Parameter	Value
Rotor outer diameter	149mm
Rotor inner diameter	100mm
Length	120mm
Steel type	M19-24G
Stacking factor	0.95
Rotor poles	12
Air gap	0.3
Insulation thickness	0.5mm
Rotor yoke thickness	11mm
Parallel branches	1
End Adjustment	5mm
Turns per pole	12
Number of strands	1
Wire size	2.743mm
Wire wrap	0.1mm
Stator outer diameter	250mm
Stator inner diameter	150mm
Stator poles	18
Stator yoke thickness	31 mm
Trigger pulse width	120°
Diode drop	5 V
Transistor drop	5 V
Frictional loss	50W
Windage loss	200W

Table 2 Different Types of Losses in SRM Acquired from RMXprt Software and Employed as Input Information for Motor-CAD Software.

Component Units	P [Input] Watts	Speed [REF] rpm	Coef. [A]	W/kg W/kg	P [speed] Watts
Loss [Armature Copper]	1067	3183	0	375.8	1067
Loss [Stator Back Iron]	334.4	3183	1.5	17.27	334.2
Loss [Stator Tooth]	167.2	3183	1.5	41.15	167.2
Loss [Rotor back iron]	334.4	3183	1.5	96.02	334.4
Loss [Windage](Ext Fan)	0	3183	3	0	0
Loss [Rotor tooth]	167.2	3183	1.5	97.12	167.2
Loss [Windage]	0	3183	3	0	0
Loss [friction-R bearing]	25	3183	1	0	25
Loss [friction- f Bearing]	25	3183	1	0	25

Figures 4 illustrate the heat distributed and managed within the motor components, i.e., stator, rotor, housing, and winding.

Figure 4 illustrates the SRM radial sectional view by Motor_CAD. Figure 5 clarifies the SRM axial sectional view using the Motor_CAD software.

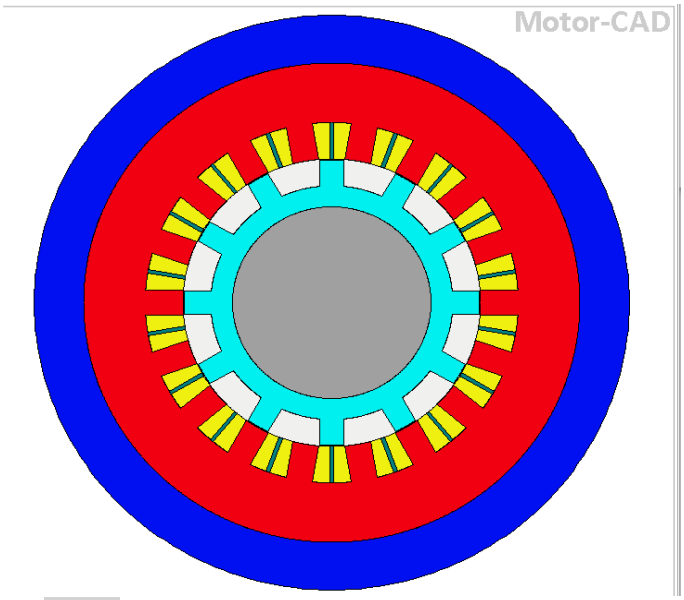

Fig. 4 SRM Radial Sectional View by Motor_CAD.

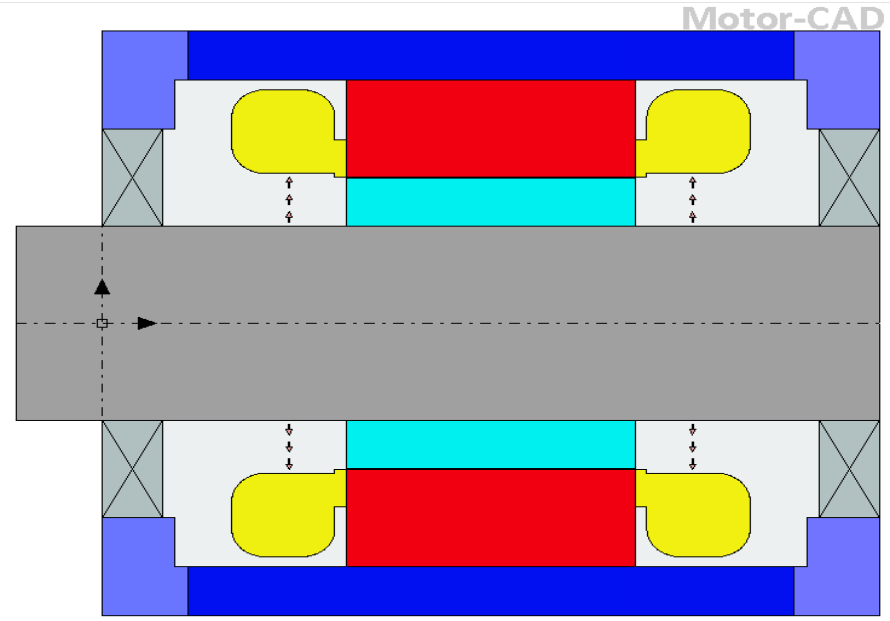

Fig. 5 SRM Axial Sectional View by Motor_CAD.

Figure 6 clarifies the thermal network for SRM in Motor-CAD. LPTN is recognized as a crucial method used in the temperature analysis of electrical machines because it provides more information regarding temperature calculation and heat transfer, as well as a quick method for scanning the distribution of the temperature within electrical machines, and allows the user to rapidly compute the alterations caused by varying parameters input. Figure 6 clarifies the SRM equivalent thermal network by Motor_CAD. Models of the LPTN include several parts, such as thermal resistance and thermal capacitance, which are combined into simplified sections that reflect complicated geometries, such as rotor teeth, stator teeth, and pole numbers. The term LPTN refers to an electrical circuit in which voltage denotes temperature, current denotes heat flow, and resistance and capacitance denote thermal resistance and capacitance. Every node in the network denotes a specific location in the motor's design and is linked to another node via a calculated thermal resistance. In SRM steady-state analysis, the thermal circuit contains thermal sources and thermal resistance connected to the motor's component nodes.

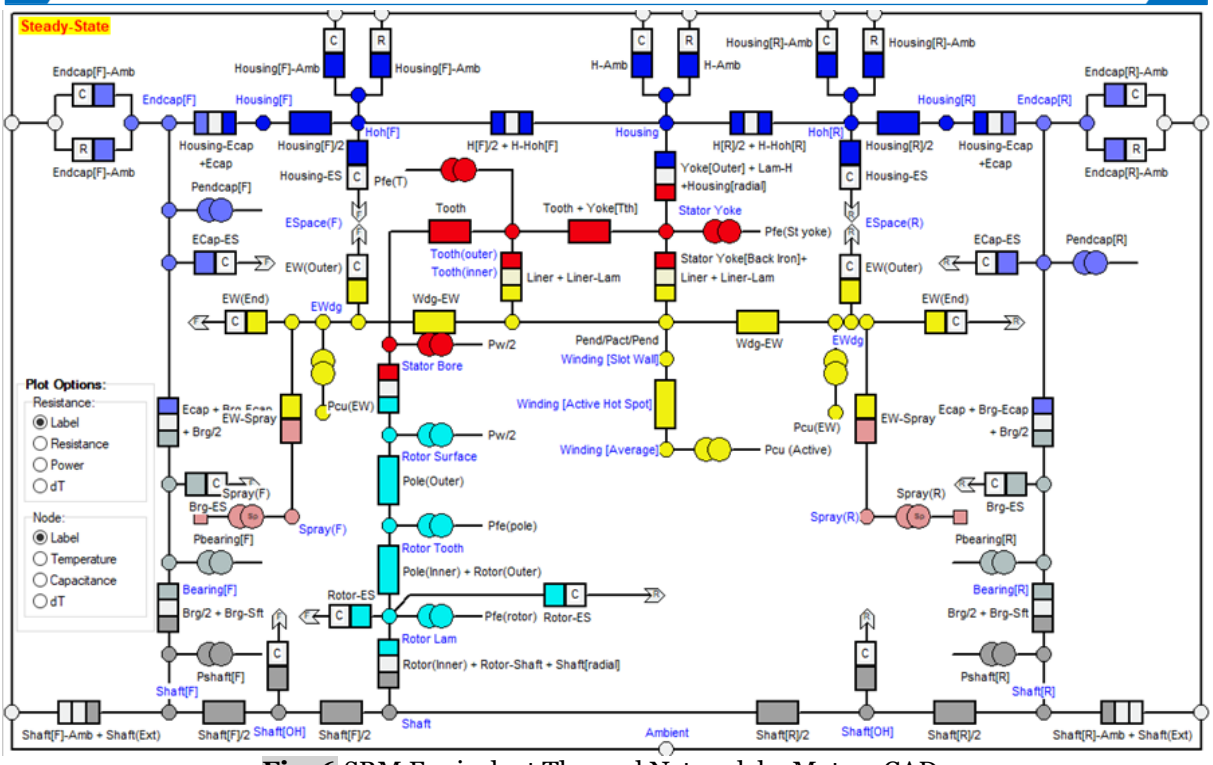

Fig. 6 SRM Equivalent Thermal Network by Motor_CAD.

4.RESULTS AND DISCUSSION

4.1.RMXprt Results

Figure 7 illustrates the relation between efficiency and speed. The maximum value of efficiency was 85.8535% and gradually reduced with increased speed. Figure 8 clarifies efficiency versus different numbers of phases, such as three-phase (stator/rotor 6/4 poles), four-phase (stator/rotor 8/6 poles), five-phase (stator/rotor 10/8 poles), six-phase (stator/rotor 12/10 poles), seven-phase (stator/rotor 14/12 poles), and three-phase (stator/rotor 18/12 poles). The maximum value of efficiency was in three-phase 18/12 poles, i.e., 85.8535%.

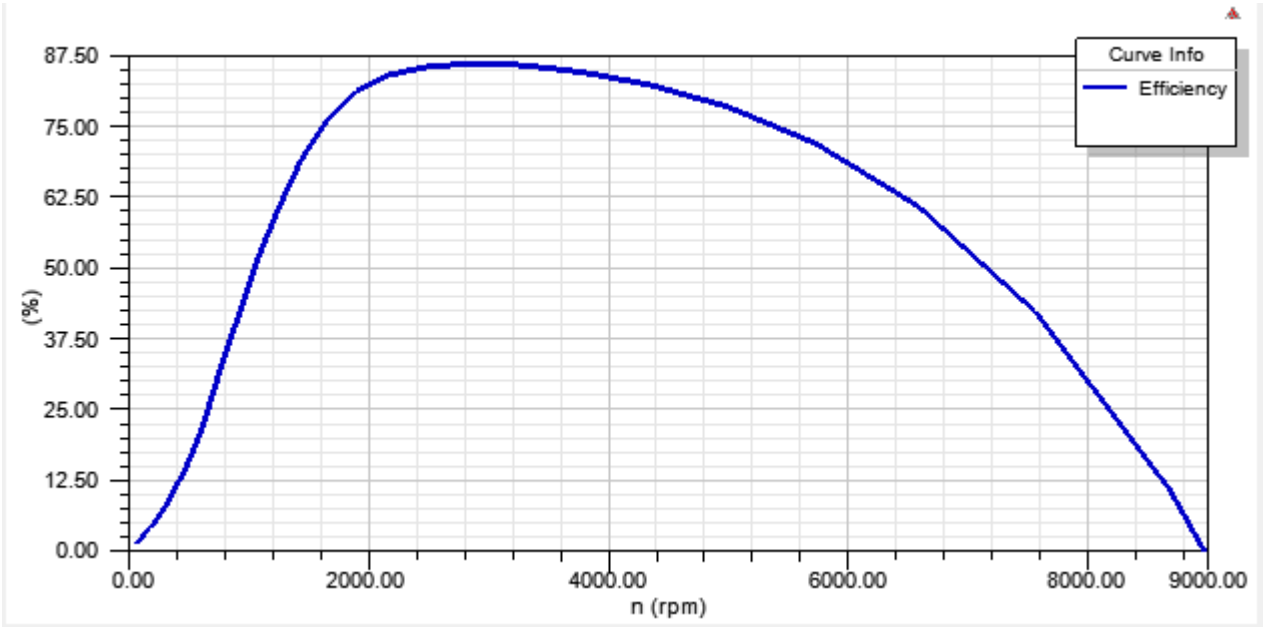

Fig. 7 SRM Efficiency Versus Speed by RMXprt.

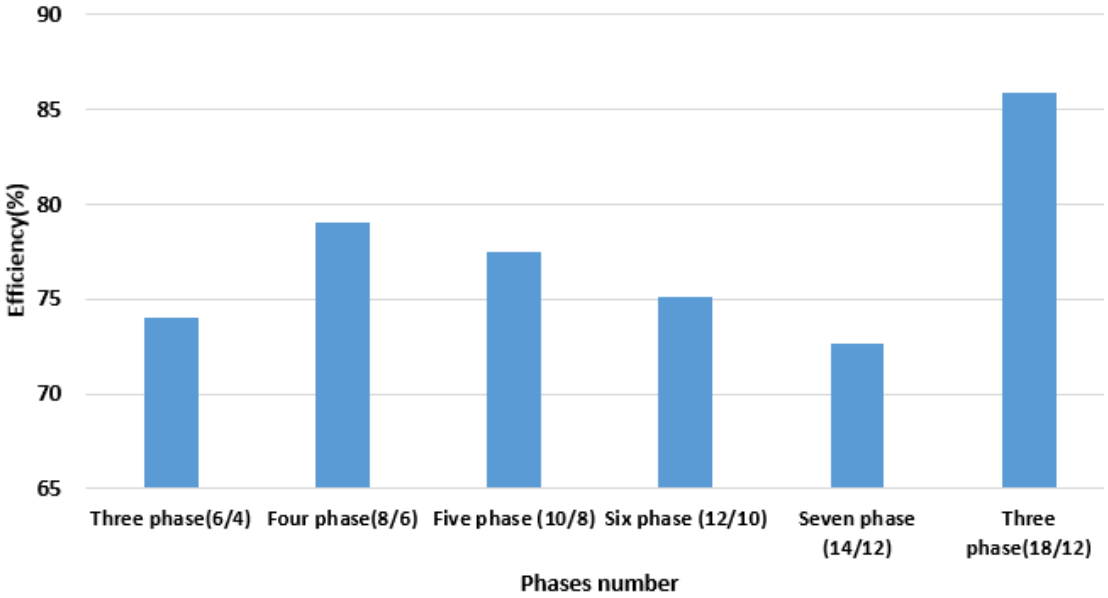

Fig. 8 Efficiency Versus different Numbers of Phases.

4.2.Motor_CAD Results

The temperature curve for SRM versus different loads is clarified in Fig. 9. Figure 9 illustrates how SRM temperature changes in response to varying loads (from no load to 1% of full load). As the load on the SRM increased, the motor typically experienced higher temperatures due to increased power dissipation and losses. The highest temperature was in winding due to a large quantity of copper losses. Monitoring this curve helps ensure the SRM operates within safe temperature limits, ensuring optimal performance and reliability and preventing overheating. Figure 10 illustrates the distribution of the temperature at full load in every component of the radial sectional view of SRM in a steady state with the spray cooling method. The housing temperature was 45 °C, representing the minimum value for temperature. While the temperature in winding was distributed in three states: the minimum value for winding temperature, i.e., 40 °C; the average temperature, i.e., 89.6 °C; and the maximum value for winding temperature, i.e., 154 °C. Figure 11 illustrates the distribution of the temperature in the SRM axial sectional view in every part, which represents the same state in the radial view.

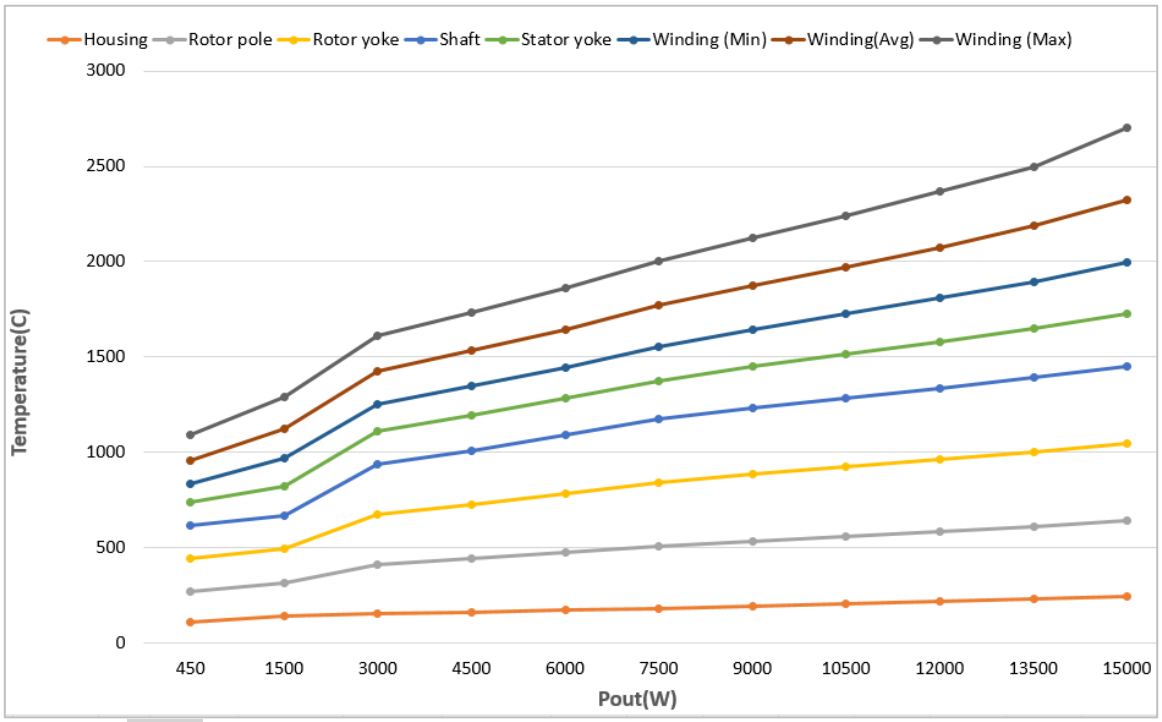

Fig. 9 The Temperature of SRM Components at Various Loading Conditions.

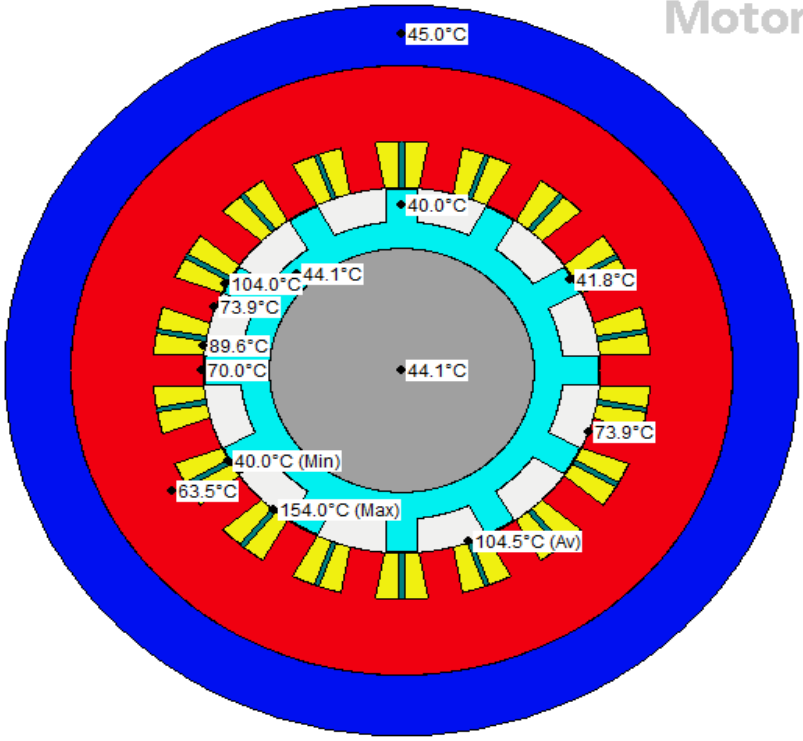

Fig. 10 Temperature Distribution in SRM Radial View by Motor_CAD.

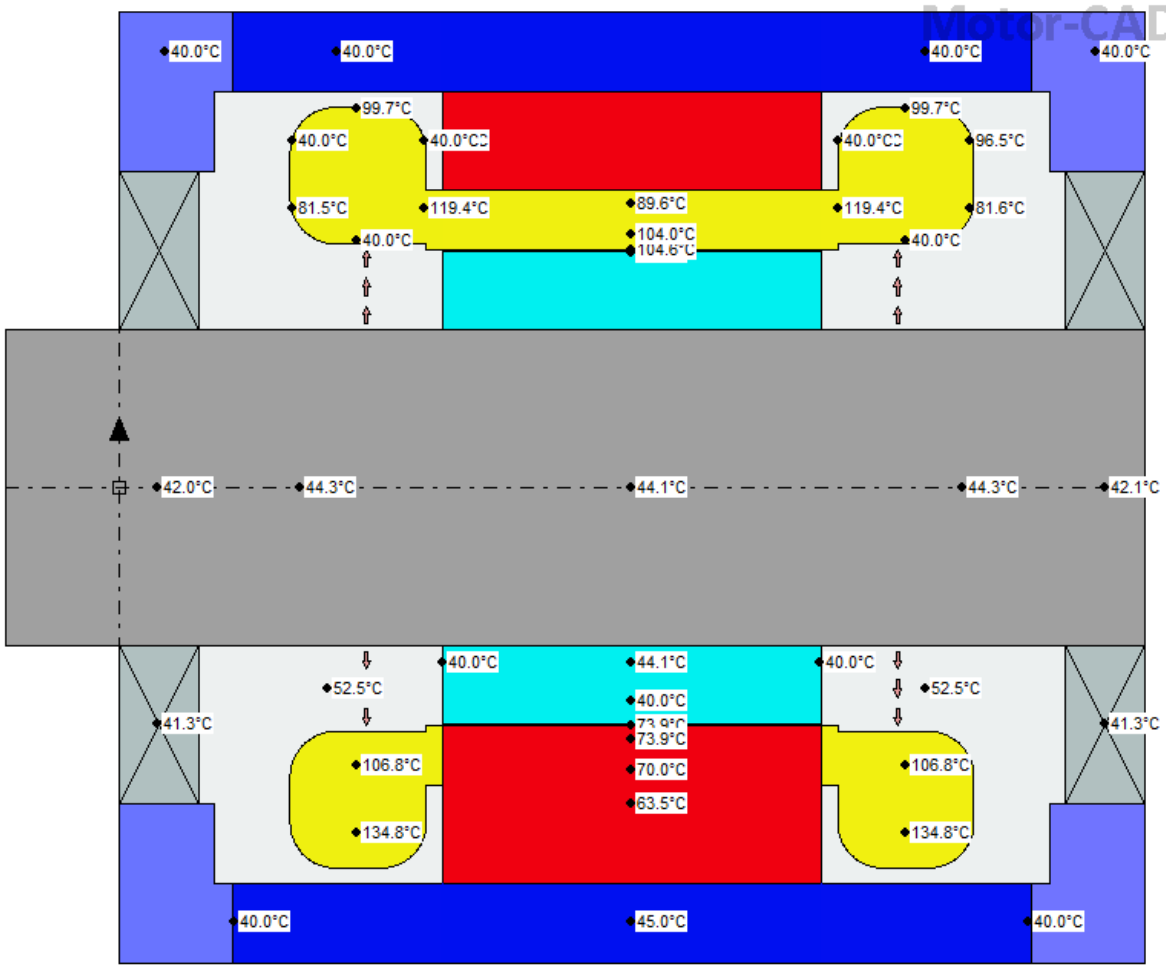

Fig. 11 Temperature Distribution in Axial Sectional View of SRM by Motor_CAD.

Figure 12 illustrates the contrast between the temperature distribution in the shaft, rotor yoke, rotor pole, housing, and the stator winding (minimum winding temperature, average winding temperature, and maximum winding temperature) in the four studied cases: case 1: without cooling, case 2: water jacket cooling (A commonly-used indirect cooling technique, water jackets enable effective heat transfer from the active part of the stator to the coolant. Features of utilizing a water jacket include a higher power-to-frame size ratio, reduced noise levels, increased efficiency, and a fully enclosed environment. Additionally, the removed heat is indirectly released into the environment.), case 3: cooling with fins (The main purpose is to enhance heat dissipation by expanding the surface area of the object, enabling it to release heat more efficiently into the surrounding air, preventing overheating and ensuring the device operates efficiently), and case 4: spray cooling (The coolant is applied to the stator core, rotor core, and end winding to lower their temperature). The analysis illustrates that case 4 had the minimum temperature inside the SRM.

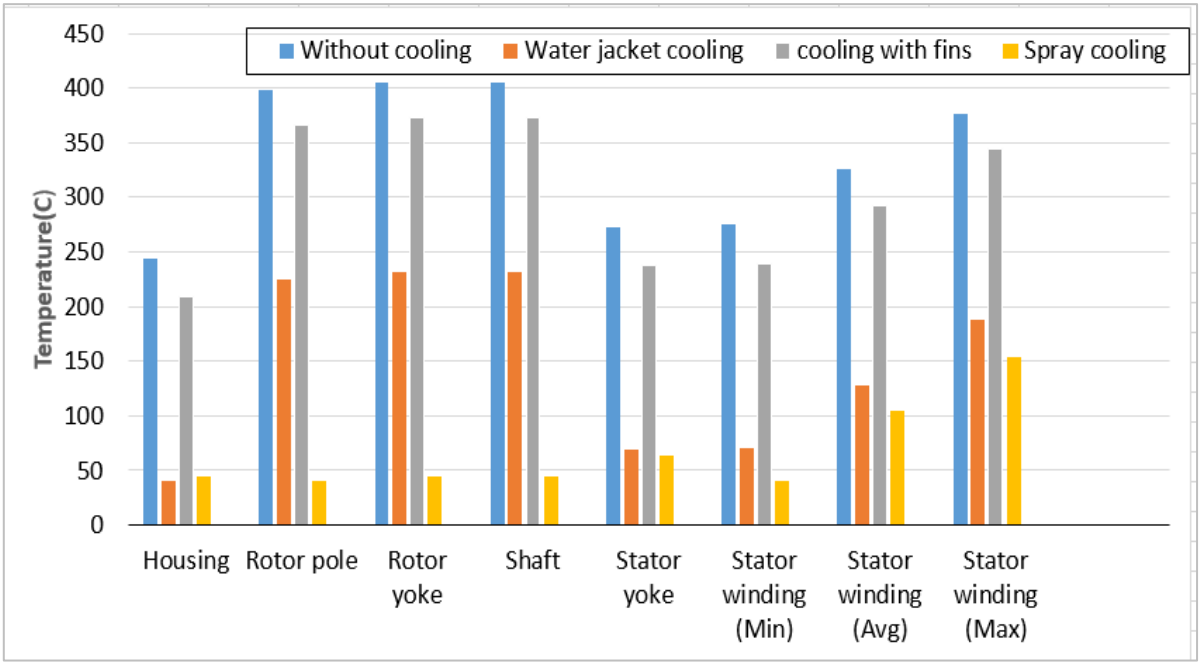

Fig. 12 Temperature Distribution in SRM with the Cooling Method.

5.CONCLUSIONS

The temperature analysis of SRM was successfully performed based on the combination of two software programs: RMXprt and Motor_CAD. The results demonstrated the maximum value of efficiency in three phases, 18/12, which was 85.8535%. These results also illustrated an increase in temperature distribution in the motor parts when the motor load increases. Furthermore, choosing the correct cooling method (using water jacket cooling, spray cooling, or housing fins) is important to reduce the SRM temperature. The results indicated that spray cooling was more effective in rapidly and efficiently reducing temperature than other methods. The present study offers a valuable guide for motor designers to improve the thermal design of SRMs without the need to produce and test costly prototype motors.

ACKNOWLEDGEMENTS

The authors express their gratitude to the Department of Computer Engineering Techniques, Al-Maarif University, for their valuable insights and feedback on this work.

NOMENCLATURE

A_s	Radiating surface area, m^2
D	Outer rotor diameter, m
Gn	Weight of the rotor, kg
h	Convection heat transfer coefficient, W/(m^2 K)
I	Current, A
k	Thermal conductivity, W/(m k)
L	Stack length, m
n	motor speed, rpm
Q_{rad}	heat radiation, W
Q_{conv}	heat convection, W
Q_{cond}	heat conduction
R	stator resistance per phase, Ω
T_o	*initial temperature, Kelvin*
T	*final temperature, Kelvin*
Greek symbols	
ρ	conductor resistivity, Ω. m
ε	Emissivity
σ	*Stefan- Boltzmann law W/(m^2 K^4)*
Subscripts	
P_T	total loss
P_{cu}	copper loss
P_{core}	core loss

REFERENCES

[1] Bilgin B, Jiang WJ, Emadi A. **Switched Reluctance Motor Drives: Fundamentals to Applications.** Boca Raton, FL; 2018.

[2] Arbab N, Wang W, Lin C, Hearron J, Fahimi B. **Thermal Modeling and Analysis of a Double-Stator Switched Reluctance Motor.** *IEEE Transactions on Energy Conversion* 2015; **30**(3):1209-1217.

[3] Elhomdy E, Liu Z, Li Z. **Thermal and Mechanical Analysis of a 72/48 Switched Reluctance Motor for Low-Speed Direct-Drive Mining Applications.** *Applied Sciences* 2019; **9**(13):2722.

[4] Pavan A, Sathyanarayanan N, Rajesh K, Lenin NC, Sivakumar R. **Thermal Investigation of a Switched Reluctance Motor.** *International Journal of Electrical Engineering* 2015; **8**(2):115-121.

[5] Bieńkowski K, Szulborski M, Sebastian Ł, Kolimas Ł, Cichecki H. **Parameterized 2D Field Model of a Switched Reluctance Motor.** *Electricity* 2021; **2**(4):590-613.

[6] Chiu HC, Jang JH, Yan WM, Shiao RB. **Thermal Performance Analysis of a 30 kW Switched Reluctance Motor.** 2017; **114**:145-154.

[7] Huang JL, Xuan Y, Zhang L, Liu TG. **Analysis on the Design and Temperature Field of Switched Reluctance Motor for Electric Vehicle.** *Journal of Physics: Conference Series* 2021; **1777**(1):12001.

[8] Jang JH, Chiu HC, Yan WM, Tsai MC, Wang PY. **Numerical Study on Electromagnetics and Thermal Cooling of a Switched Reluctance Motor.** *Case Studies in Thermal Engineering* 2015; **6**:16-27.

[9] Reis RRC, Kimpara MLM, Pinto JOP, Fahimi B. **Multi-Physics Simulation of 6/4 Switched Reluctance Motor by Finite Element Method.** *Eletrônica de Potência SOBRAEP* 2021; **26**(1):9-18.

[10] Kasprzak M, Jiang JW, Bilgin B, Emadi A. **Thermal Analysis of a Three-Phase 24/16 Switched Reluctance Machine Used in HEVs.** *IEEE Energy Conversion Congress and Exposition* 2016:1-7.

[11] Vijayakumar K, Basanth A, Karthikeyan JR, Sivakumar V, Balamurugan N, Sundaram CS. **Influence of Iron Powder Core on the Switched Reluctance Motor Performance Enhancement.** *Materials Today: Proceedings* 2020; **33**:2255-2263.

[12] Nasab PS, Moallem M, Chaharsoghi ES, Narvaez CC, Fahimi B. **Predicting Temperature Profile on the Surface of a Switched Reluctance Motor Using a Fast and Accurate Magneto-Thermal Model.** *IEEE Transactions on Energy Conversion* 2020; **35**(3):1394-1401.

[13] Abunike EC, Okoro OI, Davidson IE. **Thermal Analysis of an Optimized Switched Reluctance Motor for Enhanced Performance.** *IEEE PES/IAS PowerAfrica* 2021:1-5.

[14] Yan W, Chen H, Liu Y, Chan C. **Iron Loss and Temperature Analysis of Switched Reluctance Motor for Electric Vehicles.** *IET Electric Power Applications* 2020; **14**(11):2119-2127.

[15] Sun Y, Zhang B, Yuan Y, Yang F. **Thermal Characteristics of Switched Reluctance Motor Under Different Working Conditions.** *Progress in Electromagnetics Research M* 2018; **74**:11-23.

[16] Kartigeyan J, Ramaswamy M. **Effect of Material Properties on Core Loss in Switched Reluctance Motor Using Non-Oriented Electrical Steels.** *Journal of Magnetics* 2017; **22**(1):93-99.

[17] Kocan S, Rafajdus P. **Dynamic Model of High Speed Switched Reluctance Motor for Automotive Applications.** *Transportation Research Procedia* 2019; **40**:302-309.

[18] Kocan S, Rafajdus P, Kovacik M. **Investigation of Rotor Parameters of High Speed Switched Reluctance Motor for Automotive Application.** *Transportation Research Procedia* 2021; **55**:1003-1010.

[19] Al-Farhan SK, Yehya OSAD. **Improving the Switched Reluctance Motor Performance in Electric Vehicles Based on Changing the Parameters of the Geometry-A Review.** *Al-Rafidain Engineering Journal* 2023; **28**(2):94-112.

[20] Alattar MS, Alsammak ANBA. **Survey Paper on Six Phase Induction Motor Drive.** *Al-Rafidain Engineering Journal* 2020; **25**(1):24-31.

[21] Abbas LF, Ahmed REA, Mahmmoud ON, Gaeid K, Mokhlis HB. **Single Phasing Effects on the Behavior of Three-Phase Induction Motor.** *Tikrit Journal of Engineering Sciences* 2023; **30**(4):11-18.

[22] Mahmmoud ON, Gaeid KS, Nashi AF, Siddiqui KM. **Induction Motor Speed Control with Solar Cell Using MPPT Algorithm by Incremental Conductance Method.** *Tikrit Journal of Engineering Sciences* 2020; **27**(3):8-16.

[23] Rahman MS, Lukman GF, Hieu PT, Jeong KI, Ahn JW. **Optimization and Characteristics Analysis of High Torque Density 12/8 Switched Reluctance Motor Using**

Metaheuristic Gray Wolf Optimization Algorithm. *Energies* 2021; **14**(7):2013.

[24] Çengel YA, Ghajar AJ. **Heat and Mass Transfer Fundamentals and Applications.** McGraw-Hill Education; New York: 2015.

[25] Plešinger J. **Application of the ANSYS Development Environment for the Design of a 15 kW Switched Reluctance Motor.** České Vysoké Učení Technické v Praze; 2017.